Persico, M.; Bazinet. L. 2018. Fouling prevention of peptides from a tryptic whey hydrolysate during electromembrane processes by use of monovalent ion permselective membranes. Journal of Membrane Science, 549 : 486-494

FOULING PREVENTION OF PEPTIDES FROM A TRYPTIC WHEY HYDROLYSATE DURING ELECTROMEMBRANE PROCESSES BY USE OF MONOVALENT ION PERMSELECTIVE MEMBRANES

Mathieu Persico[a,b] and Laurent Bazinet[a,b*]

[a] *Institute of Nutrition and Functional Foods (INAF), Dairy Research Center (STELA) and Department of Food Sciences, Université Laval, Québec, QC, Canada*

[b] *Laboratory of Food Processing and ElectroMembrane Processes (LTAPEM), Université Laval, Québec, QC, Canada*

Abstract

Peptide adsorption occurring on conventional anion- and cation-exchange membranes is one of the main technological locks in electrodialysis (ED) for hydrolysate demineralization. Hence, the peptide fouling of monovalent anion (MAP) and monovalent cation (MCP) permselective membranes was studied and compared to conventional membranes (AMX-SB and CMX-SB). It appeared that the main peptide sequences responsible in fouling were TPEVDDEALEKFDK, VAGTWY and VLVLDTDYK for both anionic membranes; and ALPMHIR and TKIPAVFK for both cationic membranes. However based on the MS-MS results, the fouling was about 97-100 % lower for MAP than AMX-SB and 95-100 % lower for MCP than CMX-SB. This was explained by the differences in charge sign distribution at the membrane surface. Consequently, monovalent membranes can represent a very interesting opportunity for treatment of hydrolysate solution in electrodialytic processes by practically eliminating peptide fouling. At our knowledge, it was the first time that such a demonstration was done.

Keywords

Electrodialysis, Peptide fouling, Membrane interface, Monovalent membranes

1. Introduction

Whey protein hydrolysates (WPH) are excellent sources of bioactive peptides with functional properties such as antihypertive, antidiabetic or antibacterial activities [1, 2]. Bioactive peptides must be separated from the total WPH into smaller fractions to be used in food applications. In other cases, the WPH should be desalinated for human consumption purposes. Fractionation and purification of WPH are achieved by using membrane technologies such as ultrafiltration, nanofiltration [3, 4, 5] or electrodialysis (ED) [6]. However, peptide fouling is one of the main drawback in the membrane industry. Membrane cleaning and replacement may cost 20-30% for the pressure-driven membrane processes and 40-50% for the ED process [7, 8].

Recent studies showed that conventional food-grade anion-exchange membranes (AMX-SB) and/or cation-exchange membranes (CMX-SB) are exposed to fouling in presence of a WPH either in static [9, 10] or in hydrodynamic conditions during an ED process [11]. Fouling was mainly due to a few peptides which could establish electrostatic interactions with the membranes, and that even with no current applied. The nature of the membrane interface is a predominant parameter in peptide fouling. Thereby, fouling may be different concerning membranes having particular interfaces and different characteristics. Many studies investigated the organic fouling resistance of membranes after surface modifications by grafting specific compounds for PES and PVDF [12, 13, 14, 15, 16, 17] and for anion-exchange membranes [7, 18] using model foulants. The monovalent ion permselective membranes are another category of ion-exchange membranes allowing the migration of their oppositely-charged monovalent ions through these last while retaining the polyvalent ions. The monovalent anion permselective (MAP) membranes are made of a resin including positive charges which is covered by a very thin and highly cross-linked negatively charged layer on its surface. Inversely, monovalent cation permselective (MCP) membranes are made of resin including negative charges coated with a thin positive charge layer [19, 20]. Such layers on the membrane interface are able to separate ions with the same charge sign but different valences. The MAP are highly permeable only to monovalent anions like chloride ions whereas the MCP are highly permeable only to monovalent cations like sodium ions. With these particular layers on their interfaces, the MAP and MCP may have interesting resistance in peptide fouling. Nonetheless, there is no study dealing with the fouling of such membranes with model peptide solutions or complex peptide mixtures.

In this context, the aim of the present work was (1) to investigate the WPH fouling on MAP and MCP according to the pH, (2) to identify the characteristics and sequences of potential fouled peptide and (3) to compare that fouling in terms of quantity and peptide sequences with the conventional membranes from previous studies [9, 10, 11] carried-out with the same WPH and in the same static and ED conditions.

2. Materials and methods

2.1. Materials

Food grade Neosepta monovalent anion permselective membranes (MAP) and monovalent cation permselective membranes (MCP) were purchased from Astom (Tokyo, Japan). The HCl 1.0 N and NaOH 1.0 N were obtained from Fisher Scientific (Nepean, ON, Canada). NaCl and Na_2SO_4 were supplied by ACP Inc. (Montréal, QC, Canada). A BiPRO whey protein isolate (WPI), provided by Davisco Foods International (Eden Prairie, MN, USA) was used for the production of the whey protein hydrolysate (WPH). According to the manufacturer, the WPI composition was 92.7% of protein, 5.0% moisture and 2.3% salt (sodium, potassium, calcium, phosphorus and magnesium). Proteins in WPI consist of 68-75% β-lactoglobulin, 19-25% α-lactalbumin and 2-3% bovine serum albumin. The BiPRO WPI was hydrolyzed with pancreatic bovine trypsin (reference number: T9201) purchased from Sigma - Aldrich (St.Louis, MO, USA). Then, the hydrolysate was heated at 80°C during 30 min in order to inactivate the enzyme and avoid further breakdown of peptides [21] and freeze-dried. The final WPH was composed of 89% peptides and 11% salt. Rhodamine B dye was purchased from Sigma-Aldrich (St.Louis, MO, USA).

2.2. ED cell configuration

A 500 mL solution of 0.5% (w/w) WPH supplemented with 0.4% (w/w) NaCl (final composition: 44.5% peptides and 45.5% salt) was demineralized by ED. The ED cell was a MicroFlow type cell from ElectroCell Systems AB (Täby, Sweden) using a Xantrex power supply (HPD 60-5, QC, Canada). Four MAP and five MCP membranes of surface area of 10 cm^2 were used. The compartments defined three closed loops containing the feed solution (0.5 % WPH), the salt ion recovery (0.20 M NaCl) and the electrode-rinsing solution (0.14 M Na_2SO_4). Each closed loop was connected to an external plastic reservoir, allowing continuous recirculation at a rate of 100 mL/min for each compartment (Figure 1). The current-tension curve of this system was determined according to the method of Cowan and Brown [22] and the limiting current was reached at 11 V.

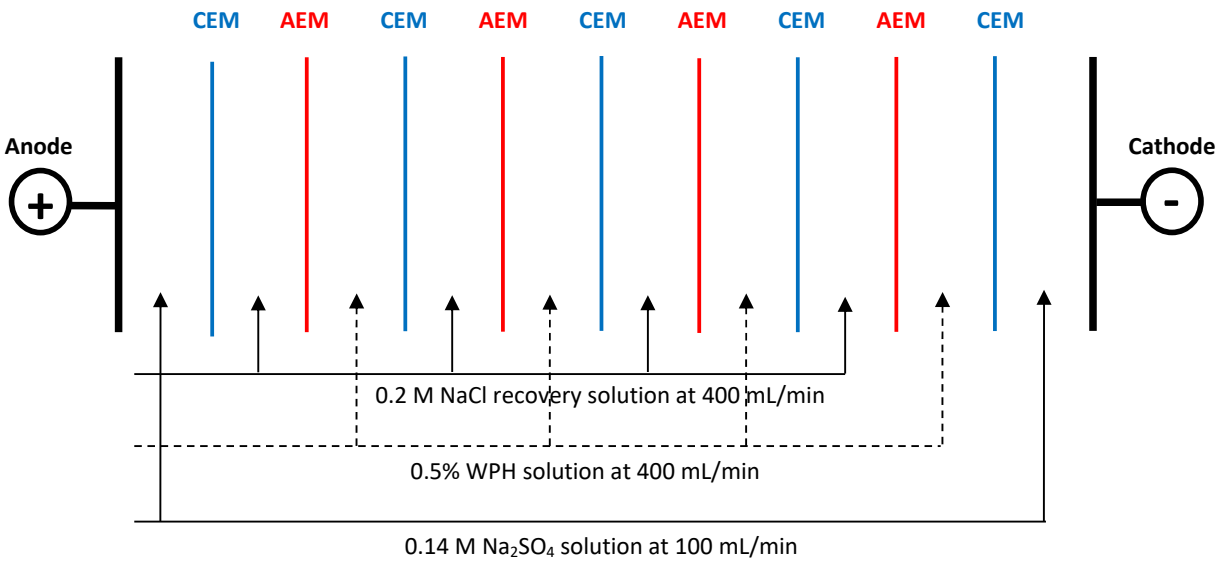

Figure 1: Electrodialysis cell configuration for demineralization of the WPH solution

2.3. Protocol

In this study, the objective was to compare and to identify the peptide fouling of monovalent ions MAP and MCP membranes with previous results of conventional AMX-SB and CMX-SB membranes in the same static [9, 10] and hydrodynamic [11] conditions and using the same model peptide solution (WPH). In static conditions, membranes were simply soaked in BiPRO WPH whereas in hydrodynamic conditions, membranes were stacked in an ED cell for demineralization.

2.3.1. Static conditions

Four virgin MAPs of 10 cm² were soaked overnight in 100 ml of a 0.5% (w/w) WPH solution after adjusting the initial pH of 8.2 at three different pH values (2, 6 and 10) in order to potentially promote the peptide-membrane interactions. Then, the membranes were rinsed with distilled water and half of them were analyzed. The second half was soaked in 20 mL of a 2.0% (w/w) NaCl desorption solution during three hours in order to remove potential peptides responsible for the fouling [23]. Afterwards, both membranes were rinsed and analyzed. The NaCl desorption solutions were recovered and freeze-dried for peptide identification by UPLC-QTOF. The same protocol was carried-out for MCP membranes. The peptide fractions previously obtained for AMX-SB [9] and CMX-SB [10] membranes were re-analysed for peptide identification in the same conditions and with the same equipment as MAP and MCP to be able to compare the UPLC-QTOF results.

2.3.2. Hydrodynamic conditions

A 0.5 % WPH solution was demineralized at pH 6 during 60 min at a voltage of 4.5 V (underlimiting current density) using an ED cell (Figure 1) as in [11]. After ED treatments, MAPs and MCPs were recovered and half of them were soaked separately in 20 mL of 2.0 % (w/w) NaCl in order to remove a potential peptide fouling. The NaCl desorption solutions were recovered and freeze-dried for peptide identification by UPLC-QTOF.

2.4. Analysis and chemicals

2.4.1. Nitrogen content of membranes

Membranes were analyzed in terms of nitrogen content using the Dumas method as described in [9]. Briefly, membrane samples were combusted at 950°C with pure oxygen and the product of combustion (gases) containing nitrogen oxides was heated to 850°C in a second furnace for complete oxidation and collected in a ballast tank. Helium was used as a carrier and nitrogen oxides were converted to molecular nitrogen and quantified.

2.4.2. Peptide concentration in NaCl desorption solutions

The peptide concentrations in the NaCl desorption solutions were determined using µBCA™ protein assay kit (Pierce Biotechnology Inc., Rockford, IL, USA). Assays were conducted as recommended by the manufacturer.

2.4.3. Peptide identification in freeze-dried NaCl desorption solutions

The freeze-dried NaCl desorption solutions were analyzed by UPLC-QTOF for peptide identification as described in [11]. Moreover, the freeze-dried NaCl desorption solutions of AMX-SB and CMX-SB in static conditions [9, 10] were reanalyzed using this new UPLC-QTOF method in order to be comparable. Freezed-dried desorption solutions were dissolved with 1.5 mL of UPLC grade water to optimize peptide concentration for mass UPLC-MS analyses. RP-UPLC analyses were performed using a 1290 Infinity II UPLC (Agilent Technologies, Santa Clara, CA, USA). The equipment consisted of a binary pump (G7120A), a multisampler (G7167B), an in-line degasser and a variable wavelength detector (VWD G7114B) adjusted to 214 nm. Diluted peptides were filtered through 0.22µm PVDF filter into a glass vial. The sample was loaded (5µL) onto an Acquity UPLC CSH 130 1.7µm C18 column (2.1mm i.d.×150mm, Waters Corporation, Milford, MA, USA). The column was operated at a flow rate of 400µL/min at 45°C. The gradient consisted of solvent A (LC-MS grade water with 0.1% formic acid) and solvent B (LC-MS grade ACN with 0.1% formic acid) starting at 2% B and ramping to 35% B in 40 min, then ramping to 85% B to 40.50 min, holding until 42 min, then back to initial conditions until 45min. A hybrid ion mobility quadrupole TOF mass spectrometer (6560 high definition mass spectrometry (IM-Q-TOF), Agilent, Santa Clara, USA) was used to identify and quantify the relative abundances of the tryptic peptides. All LC-MS/MS experiments were acquired using Q-TOF. Signals

were recorded in positive mode at Extended Dynamic Range, 2Ghz, 3200m/z with a scan range between 100–3200m/z. Nitrogen was used as the drying gas at 13.0 L/min and 150°C, and as nebulizer gas at 30psig. The capillary voltage was set at 3500 V, the nozzle voltage at 300 V and the fragmentor at 400 V. The instrument was calibrated using an ESI-L low concentration tuning mix (G1969-85000, Agilent Technologies, Santa Clara, CA, USA). Data acquisition and analysis were carried out using the Agilent Mass Hunter Software package (LC/MS Data Acquisition, Version B.07.00 and Qualitative Analysis for IM-MS, Version B.07.00 with BioConfirm Software).

2.4.4. Statistical analyses

All analyzes were performed in triplicate and three independent repetitions were done for each pH conditions and ED experiments. Data were subjected to one way analyses of variance (ANOVA). Tukey tests were also performed on data using SigmaPlot software (Version 12.0) to determine which treatment was statistically different from the others at a probability level p of 0.05.

2.4.5. Fluorescence

Fluorescence images were taken using a LSM700 Zeiss confocal microscope (Carl Zeiss Canada, North York, ON) equipped with a 20x/0.8 plan-apo objective and a 555 nm laser. The CMX-SB and MCP cationic membranes were soaked overnight in a 10^{-6} M rhodamine solution and then rinsed. Images are a collection of 5x5 tiles where each tile is a 7 images z-stack covering 42 µm in depth. Images are stitched for a final size of 1.47 mm and processed as a maximum intensity projection to remove depth irregularities in the membrane texture. Orange channel is the rhodamine dye while gray channel is the non-fluorescent transmitted light.

3. Results

3.1. Static conditions

3.1.1. Nitrogen content

Control MAP membrane contained 3.01 ± 0.01 g N/100g dry membrane (Table 1). After soaking in WPH solutions, the nitrogen content was kept constant from pH 2 to pH 6 with a very small increase trend at 10 with respective values of 3.00 ± 0.02, 3.03 ± 0.03 and 3.05 ± 0.02%. No statistical differences were observed for pH 2 and 6 vs control, while a statistical difference, close to the probability level, was observed between the control and pH 10 ($p_{pH10} = 0.046$). After soaking in NaCl solutions, nitrogen contents at pH 2, 6 and 10 did not show any significant differences with the control MAP membrane. Concerning the conventional AMX-SB [9], the nitrogen content was 2.05 ± 0.04 % for the control membrane whereas after soaking in WPH solution, it showed the same upward tendency with values of 2.00 ± 0.02, 2.15 ± 0.02 and 2.31 ± 0.02 at pH 2, 6 and 10, respectively with significant differences for pH 6 and 10.

Control MCP membrane contained 0.82 ± 0.03 g N/100g dry membrane (Table 1). After soaking in WPH solutions, the nitrogen content increased significantly to 0.88 ± 0.02 and 0.90 ± 0.04 % at pH 2 and 6 ($p_{pH2} = 0.040$ and $p_{pH6} = 0.022$), respectively and no change was observed at pH 10. After soaking in the salt solutions, the nitrogen contents were not significantly different meaning that nitrogen content returned at its initial value after desorption. Concerning the conventional CMX-SB [10], the control membrane contained 0.60 ± 0.04 %N. After soaking in WPH solution, the same tendency of fouling was observed with a maximum nitrogen content at pH 6 (1.29 ± 0.03%), lower at pH 2 (0.87 ± 0.03%) whereas no fouling was detected at pH 10 (0.67 ± 0.06%).

Table 1: Nitrogen content (%) of monovalent anion permselective (MAP) and monovalent cation permselective (MCP) membranes before and after soaking in peptides and salt solutions

Step / Membrane	MAP	MCP
Control	3.01 ± 0.01	0.82 ± 0.03
Soaked in WPH at pH 2	3.00 ± 0.02	0.88 ± 0.02
Soaked in WPH at pH 6	3.03 ± 0.03	0.90 ± 0.04
Soaked in WPH at pH 10	3.05 ± 0.03	0.83 ± 0.02
Soaked in NaCl at pH 2	2.98 ± 0.03	0.83 ± 0.05
Soaked in NaCl at pH 6	3.01 ± 0.05	0.82 ± 0.04
Soaked in NaCl at pH10	3.01 ± 0.03	0.83 ± 0.04

3.1.2. Peptide concentration in NaCl desorption solutions

After soaking MAP membranes in NaCl desorption solutions, the peptide concentration significantly increased when increasing pH with respective values of 1.4 ± 0.0, 3.9 ± 0.1, 9.0 ± 1.1 mg/L at pH 2, 6 and 10 (Table 2). Concerning the MCP membranes, the peptide concentration was significantly higher at pH 6 than pH 2 and 10 with respective values of 5.3 ± 0.3, 3.7 ± 0.6 and 2.4 ± 0.4 mg/L. Concerning the conventional membranes in the same static conditions at pH 2, 6 and 10, the peptide concentrations reported by [9, 10] were 3.2 ± 0.4, 10.7 ± 3.3 and 68.6 ± 8.3 mg/L for AMX-SB and 12.1 ± 0.4, 21.1 ± 0.6 and 5.1 ± 1.2 mg/L for CMX-SB. Therefore, it appeared that fouling was hindered by using the MAP and MCP membranes compared to conventional membranes. Indeed, fouling was 70-88 % lower for MAP than AMX-SB at pH 6 and 10 and 70-75% lower for MCP than CMX-SB at pH 2 and 6 which are the main pH conditions for fouling.

Table 2: Peptide concentration in salt solutions after monovalent anion permselective (MAP) and monovalent cation permselective (MCP) membrane desorption

Peptide concentration (mg/L)	MAP	MCP
pH 2	1.4 ± 0.0	3.7 ± 0.6
pH 6	3.9 ± 0.1	5.3 ± 0.3
pH 10	9.0 ± 1.1	2.4 ± 0.4

3.1.3. Peptide identification in salt solutions

Desorption NaCl solutions were analyzed by UPLC-QTOF for anionic membranes (AMX-SB and MAP) (Figure 2, Tables 3 and 4) and for cationic membranes (CMX-SB and MCP) (Figure 3, Tables 4 and 5). For a same pH condition, it appeared that the total signal abundance was 97-100% lower for MAP than AMX-SB and 95-100% lower for MCP than CMX-SB. Therefore, peptide fouling was eliminated or drastically lowered using monovalent ion permselective membranes instead of conventional ones.

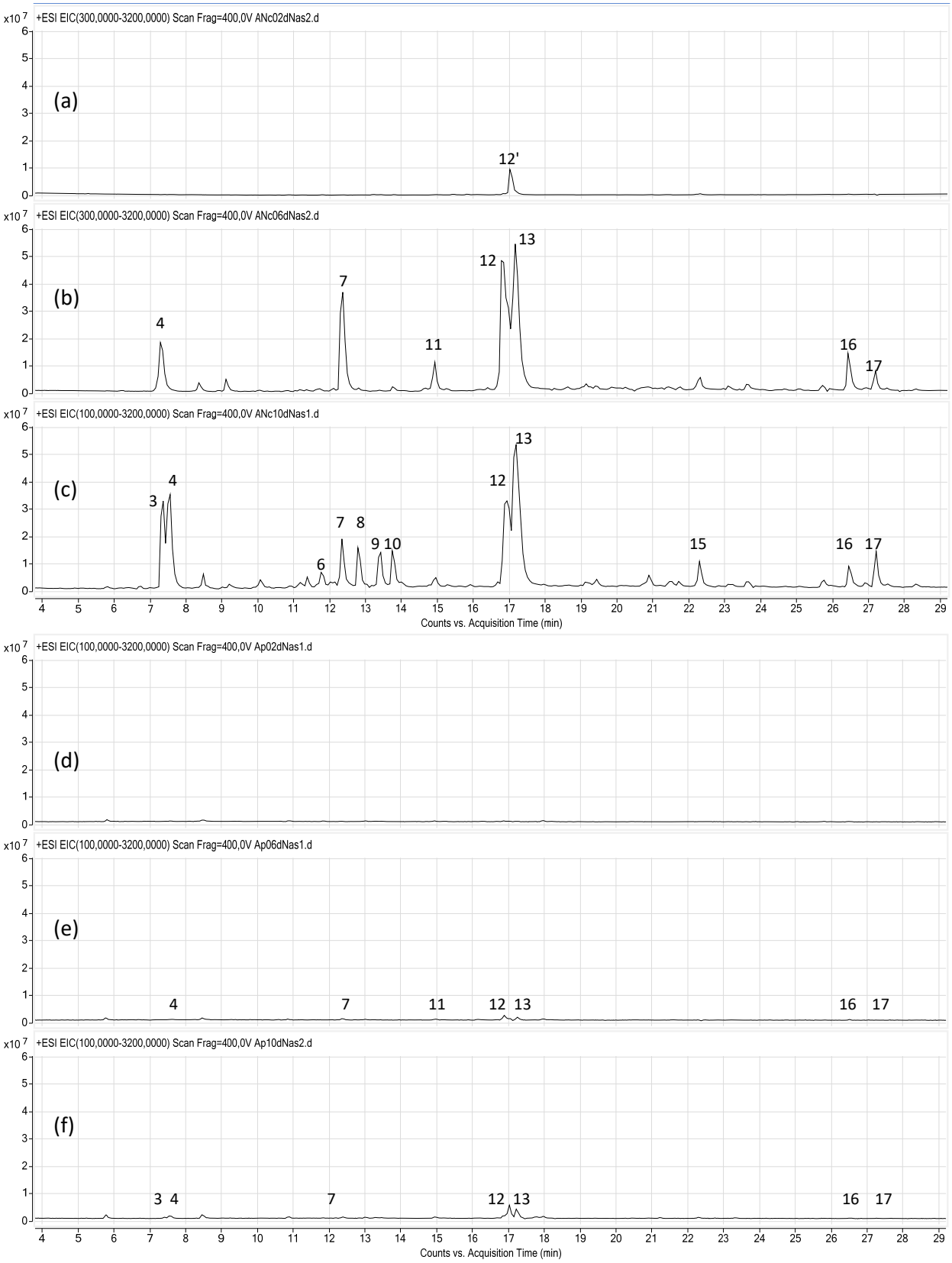

Figure 2: MS-MS profiles of NaCl desorption solutions after peptide desorption from fouled AMX-SB membranes at (a) pH 2, (b) pH 6, (c) pH 10 and from MAP membranes at (d) pH 2, (e) pH 6, (f) pH 10

Table 3: Identification of peptides found in NaCl solutions after peptide desorption from AMX-SB membranes previously soaked at pH2, 6 and 10

Peak number	Retention time (min)	Peptide sequence	Molecular weight (Da)		% abundance
			Theoretical	Observed	
pH 2 (Area: 91 ± 18 x10^{6}AU)					
12'	17.0	VAGTWY	695.3279	695.3278	> 99 %
pH 6 (Area: 1900 ± 530 x10^{6}AU)					
4	7.4	IDALNENK	915.4661	915.4658	8.2 ± 0.6
7	12.4	TPEVDDEALEK	1244.5772	1244.5769	15.9 ± 8.9
11	14.9	not identified	-	1436.6666	2.8 ± 1.1
12	16.9	TPEVDDEALEKFDK & VAGTWY	1634.7675 & 695.3279	1634.7678 & 695.3275	28.7 ± 5.1
13	17.2	VLVLDTDYK	1064.5753	1064.5748	34.1 ± 1.4
16	26.4	VYVEELKPTPEGDLEILLQK	2312.2515	2312.2529	5.2 ± 0.5
17	27.2	SLAMAASDISLLDAQSAPLR	2029.0513	2029.0514	5.1 ± 2.5
pH 10 (Area: 2500 ± 65 x10^{6}AU)					
3	7.3	GLDIQK	672.3806	672.3802	10.1 ± 1.3
4	7.5	IDALNENK	915.4661	915.4658	11.4 ± 1.8
6	11.8	LIVTQTMK	932.5365	932.5360	2.4 ± 0.8
7	12.4	TPEVDDEALEK	1244.5772	1244.5769	5.1 ± 0.8
8	12.8	not identified	-	430.2249	3.4 ± 0.6
9	13.4	IPAVFK	673.4163	673.4166	4.3 ± 0.2
10	13.8	SFNPT	564.2544	564.2901	4.3 ± 0.2
12	16.9	TPEVDDEALEKFDK & VAGTWY	1634.7675 & 695.3279	1634.7676 & 695.3275	19.5 ± 2.7
13	17.2	VLVLDTDYK	1064.5753	1064.5747	27.6 ± 2.1
15	22.3	not identified	-	750.3700	5.2 ± 3.8
16	26.5	VYVEELKPTPEGDLEILLQK	2312.2515	2312.2514	3.0 ± 1.3
17	27.2	SLAMAASDISLLDAQSAPLR	2029.0513	2029.0516	3.7 ± 1.1

Table 4: Identification of peptides found in NaCl solutions after peptide desorption from monovalent anion permselective (MAP) membranes previously soaked at pH 2, 6 and 10

Peak number	Retention time (min)	Peptide sequence	Molecular weight (Da)		% abundance
			Theoretical	Observed	
pH2 (Area : none)					
No peptide detected					
pH 6 (Area: 34 ± 5 x10^{6}AU)					
4	7.6	IDALNENK	915.4661	915.4662	4.2 ± 1.3
7	12.4	TPEVDDEALEK	1244.5772	1244.5767	12.5 ± 1.1
11	15.0	not identified	-	429.2359	7.4 ± 1.7
12	16.9	TPEVDDEALEKFDK & VAGTWY	1634.7675 & 695.3279	1634.7649 & 695.3276	48.8 ± 1.5
13	17.3	VLVLDTDYK	1064.5753	1064.5762	22.1 ± 2.6
16	26.5	VYVEELKPTPEGDLEILLQK	2312.2515	2312.2521	3.6 ± 0.0
17	27.2	SLAMAASDISLLDAQSAPLR	2029.0513	2029.0508	1.5 ± 0.2
pH 10 (Area: 77 ± 6 x10^{6}AU)					
3	7.4	GLDIQK	672.3806	672.3802	2.8 ± 0.6
4	7.5	IDALNENK	915.4661	915.4663	9.2 ± 0.6
7	12.4	TPEVDDEALEK	1244.5772	1244.5759	3.3 ± 0.7
12		TPEVDDEALEKFDK & VAGTWY	1634.7675 & 695.3279	1634.7646 & 695.3282	46.5 ± 4.2
13	17.2	VLVLDTDYK	1064.5753	1064.5750	34.1 ± 2.7
16	26.5	VYVEELKPTPEGDLEILLQK	2312.2515	2312.2520	2.4 ± 0.5
17	27.2	SLAMAASDISLLDAQSAPLR	2029.0513	2029.0517	1.6 ± 0.3

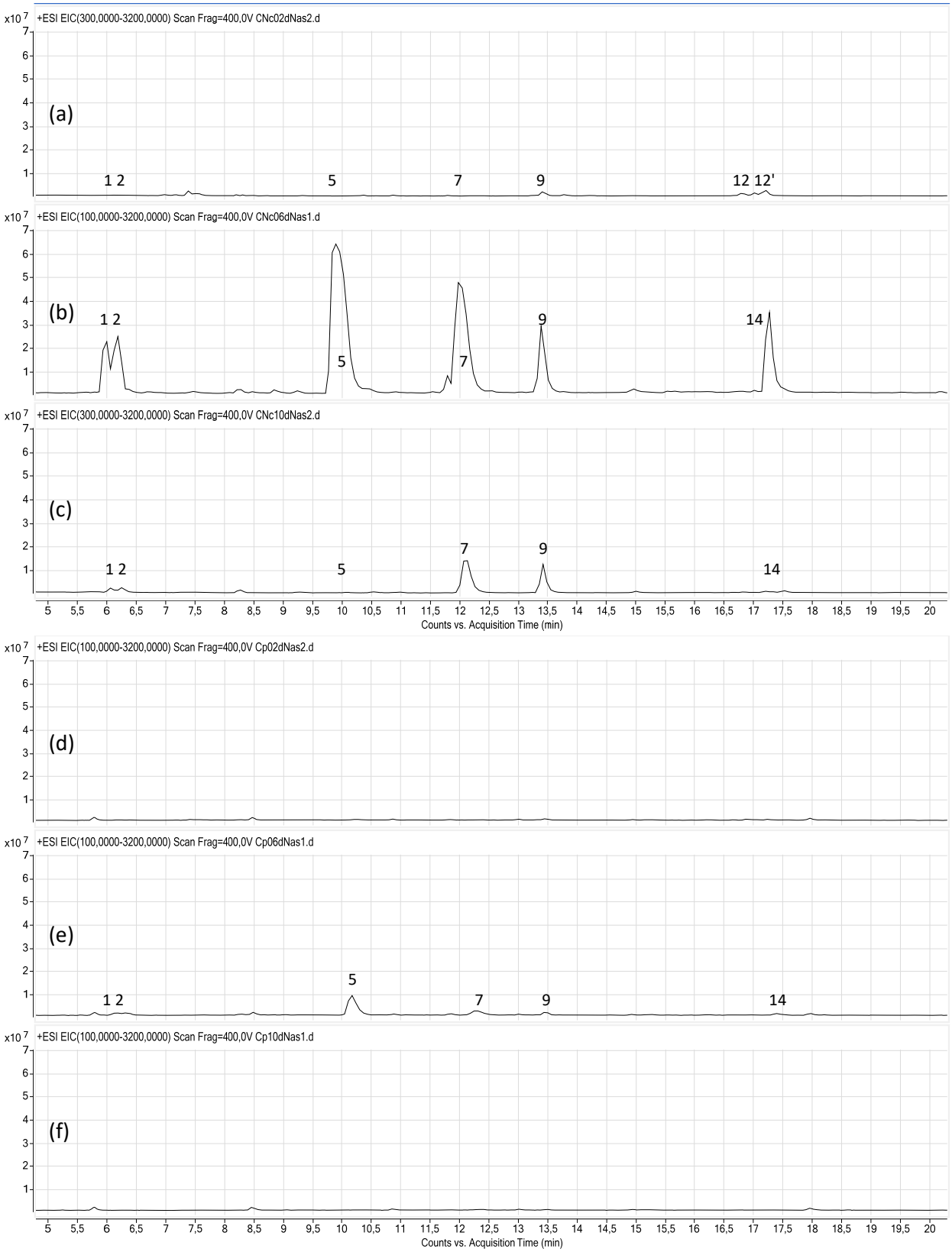

Figure 3: MS-MS profiles of NaCl desorption solutions after peptide desorption from fouled CMX-SB membranes at (a) pH 2, (b) pH 6, (c) pH 10 and from MCP membranes at (d) pH 2, (e) pH 6, (f) pH 10

Table 5: Identification of peptides found in NaCl solutions after peptide desorption from CMX-SB membranes previously soaked at pH 2, 6 and 10

Peak number	Retention time (min)	Peptide sequence	Molecular weight (Da)		% abundance
			Theoretical	Observed	
pH 2 (Area: 180 ± 170 x10^{6}AU)					
3	7.4	GLDIQK	672.3806	672.3804	14.2 ± 1.3
4	7.5	IDALNENK	915.4661	915.4658	8.9 ± 2.9
6	11.8	LIVTQTMK	932.5365	932.5365	6.4 ± 3.5
9	13.4	IPAVFK & PAVFK	673.4163 & 560.3322	673.4169 & 560.3321	20.1 ± 4.7
12	16.9	TPEVDDEALEKFDK	1634.7675	1634.7675	13.6 ± 7.3
12'	17.0	VAGTWY	695.3279	695.328	19.9 ± 7.2
pH 6 (Area: 3200 ± 530 x10^{6}AU)					
1	6.0	not identified	-	668.3426	4.6 ± 2.4
2	6.2	not identified	-	852.4633	6.2 ± 3.0
5	9.9	ALPMHIR	836.4691	836.4687	42.9 ± 5.4
7	12.0	TKIPAVFK	902.5589	902.5586	27.0 ± 0.4
9	13.4	IPAVFK & PAVFK	673.4163 & 560.3322	673.4164 & 560.3321	9.3 ± 1.2
14	17.3	TKIPAVF	774.4639	774.464	10.1 ± 0.9
pH 10 (Area: 460 ± 270 x10^{6}AU)					
1	6.1	not identified	-	668.3432	2.2 ± 1.8
2	6.3	not identified	-	852.4638	2.6 ± 1.5
5	10.8	ALPMHIR	836.4691	836.4687	13.0 ± 9.8
7	12.1	TKIPAVFK	902.5589	902.5588	52.1 ± 6.8
9	13.4	IPAVFK & PAVFK	673.4163 & 560.3322	673.416 & 560.3323	26.6 ± 3.4
14	17.5	TKIPAVF	774.4639	774.4638	3.5 ± 1.7

Table 6: Identification of peptides found in NaCl solutions after peptide desorption from monovalent cation permselective (MCP) membranes previously soaked at pH2, 6 and 10

Peak number	Retention time (min)	Peptide sequence	Molecular weight (Da)		% abundance
			Theoretical	Observed	
pH2 (Area : none)					
No peptide detected					
pH 6 (Area: 150 ± 21 x10^{6}AU)					
1	5.8	not identified	-	668.3437	4.2 ± 0.4
2	6.3	not identified	-	852.4644	12.4 ± 2.0
5	10.2	ALPMHIR	836.4691	836.4693	59.2 ± 4.1
7	12.3	TKIPAVFK	902.5589	902.5598	15.9 ± 0.6
9	13.4	IPAVFK & PAVFK	673.4163 & 560.3322	673.4178 & 560.3322	4.8 ± 2.0
14	17.4	not identified	-	262.1297	3.5 ± 0.6
pH 10 (Area : none)					
No peptide detected					

3.2. Hydrodynamic conditions

A WPH solution was demineralized at pH 6 using a voltage of 4.5 V (underlimiting current density) in an ED cell.

3.2.1. Nitrogen content

Both MAP and MCP membranes in contact with the WPH and soaked NaCl desorption solutions did not present any significant differences with their respective controls in terms of nitrogen content (Figure not shown).

Concerning the conventional AMX-SB and CMX-SB membranes, the same observation was noticed and no fouling was detected in the same conditions [11]. It was important to note that the contact duration between the membranes and the WPH in hydrodynamic condition was drastically different from those in static conditions: only one hour compared to overnight. Consequently, the contact duration in hydrodynamic conditions might have been too short to notice an extra nitrogen content, or since the MAP and MCP already contained 3.00 and 0.82 % of nitrogen in their matrices, respectively, the technique might not have been sensitive enough to notice an extra nitrogen content which was already below the lower limit of detection [24]. Furthermore, it was not possible to extend the duration of the ED treatment in order to work in the same conditions as [11] and for comparison purpose.

3.2.2. Peptide concentration in NaCl desorption solutions

In hydrodynamic conditions, the peptide concentrations in the NaCl desorption solutions were 3.0 ± 0.5 and 2.9 ± 0.4 mg/L for MAP and MCP, respectively. Concerning the conventional membranes in the same underlimiting conditions [11], it was about 13.4 and 21.8 mg/L for AMX-SB and CMX-SB, respectively.

3.2.3. Peptide identification in salt solutions

In hydrodynamic conditions, the desorption NaCl solutions did not show any peak by UPLC-QTOF profiles for both MAP and MCP (Figures not shown). Therefore, fouling was negligible/absent with permselective membranes on the contrary to conventional ones in the same underlimiting conditions. Indeed, for conventional AMX-SB, 70 % of the total abundance were due to four peptides sequences as TPEVDDEALEKFDK, VLVLDTDYK, TPEVDDEALEK and IIAEK. For conventional CMX-SB, the ALPMHIR and TKIPAVFK sequences represented 80 % of the total abundance.

3.2.4. Demineralization rate

The demineralization rate was 6.1 ± 0.4 % with the permselective MAP and MCP whereas it was 6.2 ± 1.6 by using the conventional AMX-SB and CMX-SB in the same conditions [11]. Therefore, the

demineralization rate was similar since MAP and MCP are permeable to the monovalent Na^+ and Cl^- ions.

4. Discussion

The main objective of the present study was to compare the peptide fouling between conventional and monovalent ion permselective membranes. Concerning anionic membranes, it was found that the higher the pH, the higher the peptide fouling for both permselective MAP and conventional AMX-SB [9]. However, peptide fouling was drastically decreased on the permselective ones than conventional membranes, since the total relative abundance for MAP were extremely low (about 95-100 % lower) compared to AMX-SB (Figure 2) by UPLC-MS. The nitrogen contents (by Dumas method) (Figure 4) and µBCA results confirmed this decrease but in a lower extend with respective decreases of 63-81 % and 57-88 % according to the pH conditions. Such difference in fouling decrease were due to the sensitivity of the three methods used: µBCA is a colorimetric technique and may not be as accurate as the MS-MS [11], and the analyses of nitrogen contents could not detect very low variation of nitrogen. Moreover, most of the peptide sequences found on the AMX-SB were found on the MAP membranes with the same order of proportion according to the pH but at drastically low abundances (Tables 3 and 4). At pH 6, the TPEVDDEALEK, TPEVDDEALEKFDK and VLVDTDYK sequences represented about 78 and 83 % of the total abundance for the AMX-SB and the MAP membranes, respectively. These peptides carried negatively charged D and E residues (pK_a=4.0) which could interact electrostatically with the membrane positive charges (Table 7) as previously explained in details for anion-exchange membranes by Persico *et al.* [9] according to the physicochemical properties of the peptides, the amino acid place into the peptide sequence and the 3D structure of the peptides. Concerning the cationic membranes, fouling was the highest at pH 6, lower at pH 2 and none at pH 10 for both permselective MCP and conventional CMX-SB [10]. Once again, peptide fouling was really low with a total relative abundance of peptides for MCP decreased of about 95-100 % lower compared to CMX-SB (Figure 3). Fouling was 79-100 % lower for MCP than CMX-SB by comparing the nitrogen content (Figure 4) and 44-75 % lower for MCP according to the µBCA results. The identified sequences were the same between both membranes excepted at pH 2 and 10 for MAP probably because the peptide abundances were too low (Tables 5 and 6). At pH 6, the TKIPAVFK, ALPMHIR, IPAVFK and PAVFK sequences represented about 73 and 80 % of the total abundance for the CMX-SB and the MCP membranes, respectively. These peptides carried positively charged K (pK_a=10.5) and R (pK_a=12.5) residues which interacted electrostatically with the negative groups of the CMX-SB and MCP membranes (Table 7) as explained in details for cation-exchange membranes by Persico *et al.* [10].

Table 7: Global charges of peptides recovered in the desorption solutions

Anion-exchange membranes		Cation-exchange membranes	
Peptide sequence	**Global charge**	**Peptide sequence**	**Global charge**
GLDIQK	0	ALPMHIR	+ 1
IDALNENK	- 1	TKIPAVFK	+ 2
TPEVDDEALEK	- 4	IPAVFK	+ 1
VAGTWY	0	TKIPAVF	+ 1
TPEVDDEALEKFDK	- 4		
VLVLDTDYK	- 1		
VYVEELKPTPEGLEILLQK	- 2		
SLAMAASDISLLDAQSAPLR	- 1		

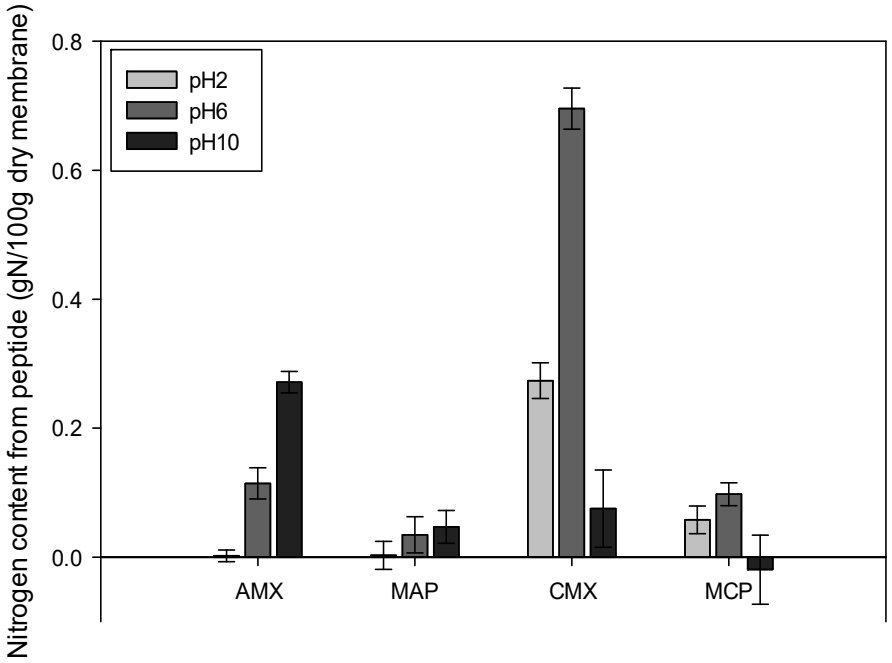

Figure 4: Nitrogen content coming from fouled peptides on the different membranes compared with already published data in static conditions (Adapted from [9, 10])

This decrease in fouling for permselective MAP and MCP membranes is due to the presence of a thin layer oppositely charged with their respective matrix. Indeed, a fluorescence capture using a positively charged rhodamine B of the MCP surface is shown and compared with CMX-SB (Figure 5). It appeared that the CMX-SB was totally recovered by the rhodamine B in yellow which demonstrates that its charges were homogeneously distributed. However, most of the MCP surface did not interact

with the rhodamine. Therefore, its thin layer would have repulsed peptides which could potentially interact with the rest of its matrix underneath. Nonetheless, permselective membranes were fouled by peptides oppositely charged to the charges inside their respective matrix. Therefore, these peptides interacted with the membrane charges located under the thin layer. The rhodamine B was present all over the surface of the conventional CMX-SB whereas it was only detected in scattered cavities (probably crosslinking polymers) for MCP. Therefore, the thin layer over the matrix of MCP was not homogenous and did not cover completely its matrix. Consequently, a few peptides could get adsorbed into the cavities where the charges were reachable.

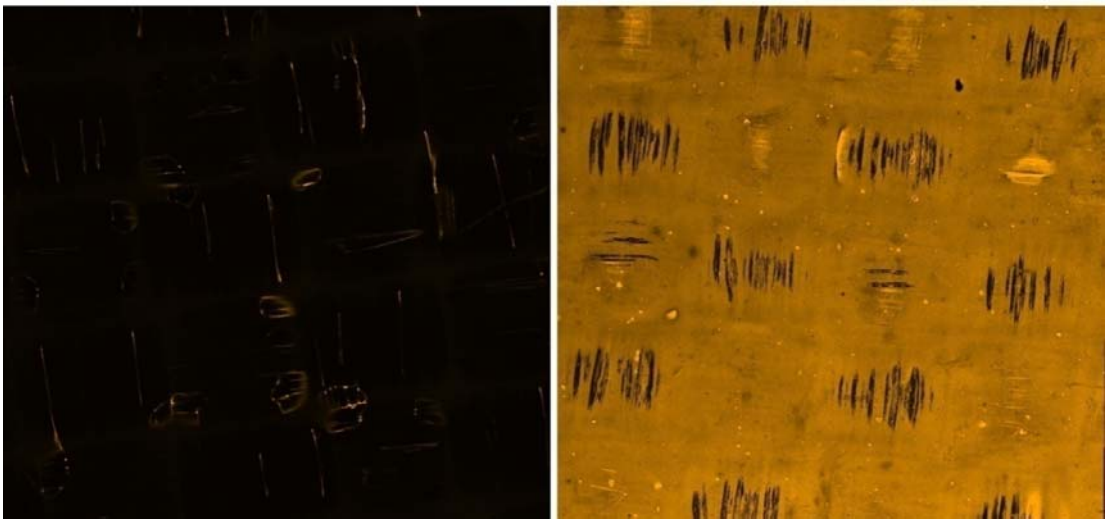

Figure 5: Fluorescent MCP (left) and CMX (right) surfaces using rhodamine B

The peptide fouling was especially different for the cationic membranes at pH 6 with 0.70 ± 0.03 and 0.10 ± 0.02 gN/100g for CMX-SB and MCP, respectively. Indeed for CMX-SB, it was hypothesized that a first layer of peptides interacted electrostatically with the negative membrane charges and then, a second layer of peptides interacted hydrophobically with the peptides from the first one. Concerning the MCP, since there is a thin positive membrane layer onto its matrix, most of peptides could not get adsorbed so the first electrostatic layer of peptides was very low. Consequently, the second hydrophobic layer could not take place due to the lack of required peptides from the first layer. The same mechanism of action and explanation should applied to the MAP membrane although we did not find an efficient negatively-charged fluorophore to be used for anionic membranes.

Conclusion

Peptide fouling over monovalent ion permselective membranes was studied and compared with conventional ones. Monovalent permselective membranes can be used to avoid fouling in ED processes working with peptide solutions. Indeed, it was demonstrated that peptide fouling was

overwhelmingly reduced using monovalent permselective membranes. As expected, the presence of a thin layer oppositely charged to the membrane matrix modified the equilibrium between peptides and the membrane surface. Nonetheless, since the thin layer did not completely cover the membrane matrix, a few peptides could reach it. In static conditions during 24 h, fouling was very low with permselective membranes compared to conventional ones. In hydrodynamic conditions, no more fouling was detected after 60 min of demineralization with monovalent selective membranes in comparison with conventional ones.

Acknowledgements

The financial support of the Natural Sciences and Engineering Research Council of Canada (NSERC) is acknowledged. This work was supported by the NSERC Industrial Research Chair on Electromembrane processes aiming the ecoefficiency improvement of biofood production lines [Grant IRCPJ 492889-15 to Laurent Bazinet] and the NSERC Discovery Grants Program [Grant SD 210829409 to Laurent Bazinet]. The authors thank Alexandre Bastien and Jacinthe Thibodeau, research professionals at Université Laval, for their great technical implication in this project.

References

1. Korhonen, H. Milk-derived bioactive peptides : From science to applications. *Journal of Functional Foods* **2009,** *1* (2), 177-187.
2. Hernández-Ledesma, B.; García-Nebot, M. J.; Fernández-Tomé, S.; Amigo, L.; Recio, I. Dairy protein hydrolysates: Peptides for health benefits. *International Dairy Journal* **2013**, 1-19.
3. Butylina, S.; Luque, S.; Nyström, M. Fractionation of whey-derived peptides using a combination of ultrafiltration and nanofiltration. *Journal of Membrane Science* **2006,** *280* (1–2), 418-426.
4. Fernández, A.; Zhu, Y.; FitzGerald, R. J.; Riera, F. A. Membrane fractionation of a β-lactoglobulin tryptic digest: effect of the membrane characteristics. *Journal of Chemical Technology & Biotechnology* **2014,** *89* (4), 508-515.
5. Arrutia, F.; Rubio, R.; Riera, F. A. Production and membrane fractionation of bioactive peptides from a whey protein concentrate. *Journal of Food Engineering* **2016,** *184* (Supplement C), 1-9.
6. Greiter, M.; Novalin, S.; Wendland, M.; Kulbe, K.-D.; Fischer, J. Desalination of whey by electrodialysis and ion exchange resins: analysis of both processes with regard to sustainability by calculating their cumulative energy demand. *Journal of Membrane Science* **2002,** *210* (1), 91-102.
7. Grebenyuk, V. D.; Chebotareva, R. D.; Peters, S.; Linkov, V. Surface modification of anion-exchange electrodialysis membranes to enhance anti-fouling characteristics. *Desalination* **1998,** *115* (3), 313-329.
8. Mikhaylin, S.; Bazinet, L. Fouling on ion-exchange membranes: Classification, characterization and strategies of prevention and control. *Advances in Colloid and Interface Science* **2016,** *229*, 34-56.

9. Persico, M.; Mikhaylin, S.; Doyen, A.; Firdaous, L.; Hammami, R.; Bazinet, L. How peptide physicochemical and structural characteristics affect anion-exchange membranes fouling by a tryptic whey protein hydrolysate. *Journal of Membrane Science* **2016,** *520*, 914-923.
10. Persico, M.; Mikhaylin, S.; Doyen, A.; Firdaous, L.; Hammami, R.; Chevalier, M.; Flahault, C.; Dhulster, P.; Bazinet, L. Formation of peptide layers and adsorption mechanisms on a negatively charged membrane surface. *Journal of Colloid and Interface Science* **2017**.
11. Persico, M.; Mikhaylin, S.; Doyen, A.; Firdaous, L.; Nikonenko, V.; Pismenskaya, N.; Bazinet, L. Overlimiting conditions prevent peptide fouling on ion-exchange membranes during electrodialysis. *Journal of Membrane Science* **2017**.
12. Yune, P. S.; Kilduff, J. E.; Belfort, G. Fouling-resistant properties of a surface-modified poly(ether sulfone) ultrafiltration membrane grafted with poly(ethylene glycol)-amide binary monomers. *Journal of Membrane Science* **2011,** *377* (1), 159-166.
13. Li, Q.; Bi, Q.-Y.; Liu, T.-Y.; Wang, X.-L. Resistance to protein and oil fouling of sulfobetaine-grafted Poly(vinylidene Fluoride) hollow fiber membrane and the electrolyte-responsive behavior in NaCl solution. *Applied Surface Science* **2012,** *258* (19), 7480-7489.
14. Li, Q.; Bi, Q.-Y.; Zhou, B.; Wang, X.-L. Zwitterionic sulfobetaine-grafted poly(vinylidene fluoride) membrane surface with stably anti-protein-fouling performance via a two-step surface polymerization. *Applied Surface Science* **2012,** *258* (10), 4707-4717.
15. Liu, J.; Shen, X.; Zhao, Y.; Chen, L. Acryloylmorpholine-Grafted PVDF Membrane with Improved Protein Fouling Resistance. *Industrial & Engineering Chemistry Research* **2013,** *52* (51), 18392-18400.
16. Zhu, L.-J.; Zhu, L.-P.; Jiang, J.-H.; Yi, Z.; Zhao, Y.-F.; Zhu, B.-K.; Xu, Y.-Y. Hydrophilic and anti-fouling polyethersulfone ultrafiltration membranes with poly(2-hydroxyethyl methacrylate) grafted silica nanoparticles as additive. *Journal of Membrane Science* **2014,** *451* (Supplement C), 157-168.
17. Shen, X.; Yin, X.; Zhao, Y.; Chen, L. Improved protein fouling resistance of PVDF membrane grafted with the polyampholyte layers. *Colloid and Polymer Science* **2015,** *293* (4), 1205-1213.
18. Mulyati, S.; Takagi, R.; Fujii, A.; Ohmukai, Y.; Maruyama, T.; Matsuyama, H. Improvement of the antifouling potential of an anion exchange membrane by surface modification with a polyelectrolyte for an electrodialysis process. *Journal of Membrane Science* **2012,** *417–418*, 137-143.
19. Abdu, S.; Martí-Calatayud, M.-C.; Wong, J. E.; García-Gabaldón, M.; Wessling, M. Layer-by-Layer Modification of Cation Exchange Membranes Controls Ion Selectivity and Water Splitting. *ACS Applied Materials & Interfaces* **2014,** *6* (3), 1843-1854.
20. Van der Bruggen, B.; Koninckx, A.; Vandecasteele, C. Separation of monovalent and divalent ions from aqueous solution by electrodialysis and nanofiltration. *Water Research* **2004,** *38* (5), 1347-1353.
21. Suwal, S.; Rozoy, É.; Manenda, M.; Doyen, A.; Bazinet, L. Comparative Study of in Situ and ex Situ Enzymatic Hydrolysis of Milk Protein and Separation of Bioactive Peptides in an Electromembrane Reactor. *ACS Sustainable Chemistry & Engineering* **2017,** *5* (6), 5330-5340.
22. Cowan, D. A.; Brown, J. H. Effect of Turbulence on Limiting Current in Electrodialysis Cells. *Industrial & Engineering Chemistry* **1959,** *51* (12), 1445-1448.
23. Kisley, L.; Chen, J.; Mansur, A. P.; Dominguez-Medina, S.; Kulla, E.; Kang, M. K.; Shuang, B.; Kourentzi, K.; Poongavanam, M.-V.; Dhamane, S.; Willson, R. C.; Landes, C. F. High ionic strength narrows the population of sites participating in protein ion-exchange adsorption: A single-molecule study. *Journal of Chromatography A* **2014,** *1343* (0), 135-142.
24. ISO 14891:2002 (IDF 185:2002) - Milk and milk products -- Determination of nitrogen content -- Routine method using combustion according to the Dumas principle.